AUT Journal of Electrical Engineering

AUT J. Elec. Eng., 50(2) (2018) 121-128
DOI: 10.22060/eej.2018.13703.5181

Response of A Saline Solution Containing A Macromolecule To An External Electric Field

Sh. Nikzad[1], H. Noshad[1*], M. Saviz[2]

[1] Department of Energy Engineering and Physics, Amirkabir University of Technology, Tehran, Iran.
[3] Assistant Professor, Department of Biomedical Engineering, Amirkabir University of Technology Tehran, Iran

ABSTRACT: The dynamical behavior of a model for body fluids in response to an external electric field is computationally investigated for communication frequencies. The effect of an applied potential difference between two electrodes in a saline solution containing a rodlike macromolecule is studied by solving the Poisson and ion continuity equations simultaneously using the finite element method (FEM). Examples of such macromolecules are stiff fragments of DNA or actin filaments. The electric field of 66 Vm^{-1} is considered to be applied along the symmetry axis of the system with a frequency of 1 GHz. For times larger than a few microseconds, the aggregation of the counter ions around the macromolecule decreases. This result is consistent with the experimental evidence reported in the literature. In order to reach sufficient accuracy of the model, the effect of the electroosmotic flow is investigated on the counter ion number density and on the permittivity of the system, which shows negligible effect. The real and imaginary parts of effective complex permittivity are obtained as 73.43 and 3.61, respectively, which is in agreement with the experimental limits obtained for protein solution. It is notable that the analysis is applicable to the Global System for Mobile communications (GSM) which operates in the GHz frequency band.

Review History:
Received: 13 November 2017
Revised: 23 September 2018
Accepted: 8 October 2018
Available Online: 20 October 2018

Keywords:
Electric Field
Biomolecule
Counter Ion
Permittivity

1- Introduction

Currently, the biological effects of nonionizing electromagnetic fields (EMFs) from radio to microwave frequencies have been the subject of numerous experimental and theoretical studies. For many years, hyperthermia and the related radiometry have been a major subject of interest in investigating biological effects of microwaves [1-5]. More recently, however, other subjects have received much attention, in particular electromagnetic (EM) energy absorption in human bodies. For instance, one can indicate interaction of microwaves with the nervous system [6], influence of the fields of mobile phones on membrane channels [7] and molecular effects [8].

Electromagnetic fields are able to influence the solutions containing proteins or may interact directly or indirectly with the protein macromolecule. For instance, the firefly luciferase is a protein which its emission spectrum is sensitive to its structure as well as the environmental conditions. It has been shown that the EMF exposure of luciferase results in its enhanced activity, possibly due to reduced aggregation of counter-ions [9]. In fact, the counter ion cloud around the macromolecule (Polyelectrolyte) might be perturbed, following which the possibility of conformational changes in the structure of the proteins cannot be neglected by EMF exposure [10]. A theoretical study of this effect is consequently necessary in order to understand related mechanisms. As regards the present study, we anticipate that the applied electric field can lead to the decrease of Debye shielding in the environment of the protein.

The influence of external electric fields on polyelectrolytes has been studied by various experimental and theoretical methods [11-16]. A typical dielectric spectrum has been obtained by merging dielectric spectra measured for DNA aqueous solutions in the range from 1 kHz to 70 GHz by [17] and the Mandel group [18]. In this paper, a time-dependent potential difference is applied between two parallel-plate capacitive coupling electrodes. The effect of the potential difference on the response in a saline solution containing a rod-like macromolecule is studied using the FEM. It is notable that the finite element analysis of any problem involves four steps [19]: discretization of the region of interest into a number of elements, derivation of equations for a typical element, assembling all elements in the region and finally solving the set of equations. The sinusoidal electric field is applied in the z direction with an intensity of 66 Vm^{-1} at the frequency of 1 GHz. This field intensity can be plausibly produced by a mobile phone working in GSM-900 frequency band and at a standard specific absorption rate (SAR) of 1.6 W/kg. It is notable that the analysis is applicable to the Global System for Mobile communications (GSM) which operates in the GHz frequency band. As the intensity of the electric field is not large enough, the dielectric constant behaves linearly, which means that it is independent of the intensity of the electric field. In other words, the dielectric coefficient can be properly considered to act in the linear regime. Without loss of generality, the computations are made for a geometry including one macromolecule. Considering a macromolecule means that the other molecules are far from the macromolecule so that their presence or absence has not influence on the charge distribution of that macromolecule. In the other words, good agreement is expected to the experimental results only

Corresponding author, E-mail: hnoshad@aut.ac.ir

for the dilute solution of protein in this work. Furthermore, in this model it is assumed that the macromolecule is rod-like. Examples of such macromolecules are stiff fragments of DNA or actin filaments [20], but the obtained qualitative behavior can be generalized to many kinds of macromolecules. Moreover, the wavelength is considered large, compared to the dimensions of the system. Therefore, quasi-static EMF theory can be properly applied.

It is worth noting that in the paper [21], the time-dependent development of electric double-layers (ionic sheaths) in saline solutions is studied by solving the sodium and chlorine ion continuity equations, coupled with Poisson's equation in one dimension. The time scales have been predicted for the formation of double-layers. In this paper, the effect of an applied potential difference between two electrodes in a saline solution containing a rod-like macromolecule is studied by solving simultaneously the Poisson and ion continuity equations in two dimensions using the finite element method (FEM). As a result, the time evolution of the charge density distribution is computed around the macromolecule.

Furthermore, in the paper [22] it was indicated that electroosmotic flow might play an important role in the intracellular transport of biomolecules. The effect of the electroosmotic flow was denoted to be quite substantial so that the flux of the messenger proteins increases onto the nucleus up to 4fold relative to pure diffusion. In this work, in order to reach sufficient accuracy of the model we study its influence on the number density of the counter ions around the macromolecule as well as the permittivity of the system. As far as we know, the results obtained in this work have not been reported in the literature previously.

This article is organized as follows. First, the theory describing the model is explained. Afterwards, the obtained numerical results are presented. Finally, the paper is ended by a conclusion.

2- Theoretical description and model

2- 1- Continuity equation for time dependent behavior

In this study, it has been assumed that the electrolyte consists of two types of ions with opposite polarities. The potential difference is applied between two electrodes. When an ionic material is dissolved in a liquid of high dielectric constant, the ions are dissociated and they can move in opposite directions due to the external electric field. By applying a voltage difference to the electrodes, the counter ions move near the electrodes, whereas the co-ions will be repelled from the electrodes. As the ions cannot penetrate the electrode surface, concentration of the accumulated counter ions in the vicinity of electrodes will be high in comparison with that of the other parts in the liquid. This movement results in the formation of an ion electric double-layer (EDL) with a steeply rising electric field as the ion approaches the electrode surface [23]. A similar phenomenon occurs around a charged macromolecule.

To obtain time dependent distributions of the ion densities, the individual continuity equations for positive and negative ions coupled with Poisson's equation are simultaneously solved, using a small time step. For stability of the computations, the time step is limited by the Courant–Friedrics–Levy condition [24]. The Poisson and continuity equations are used for computing the potential and density distributions of the positive and negative ions, respectively.

It is worth noting that by obtaining the scalar and vector retarded potentials, the time dependent electric and magnetic fields can be generally calculated by considering the retardation effect. These fields are well known to the Jefimenko's equations [25, 26]. For the systems with the dimensions much smaller than the wavelength, i.e. $l \ll \lambda$ the electric and magnetic fields are reduced to the quasi-static fields.

For the distribution of the considered electrical charge with the nanometer dimensions, we have

$$l \ll \frac{c}{\nu} \Rightarrow 10^{-9}\,\mathrm{m} \ll 0.3\,\mathrm{m}$$

where c is the speed of light and ν shows the frequency of our problem that is equal to 1 GHz. In other words, wavelength is considered large, compared to the dimensions of the system. As a conclusion, the retarded effects and the electromagnetic radiation can be fully ignored. Therefore, quasi-static EMF theory can be properly applied and we have

$$\nabla \times \mathbf{E}(\mathbf{r},t) = 0.$$

which leads to

$$\mathbf{E}(\mathbf{r},t) = -\nabla \Phi(\mathbf{r},t).$$

Hence, the Poisson's equation is fully suitable for the analysis of the problem obtaining $\Phi(\boldsymbol{r},t)$.

The Poisson equation is formulated as follows [26]

$$\nabla^2 \Phi = -\frac{e}{\varepsilon_r \varepsilon_0}\left(\rho_{Na} - |\rho_{Cl}|\right), \tag{1}$$

where ε_r denotes the relative dielectric constant.

The continuity equation is derived from the zeroth velocity moment of the Boltzmann equation.

The continuity equations are formulated for the ion density distributions, which can be presented for sodium and chlorine ions as follows [21]

$$\frac{\partial \rho_{Na}}{\partial t} + \nabla . \boldsymbol{\Gamma}_{Na} = 0 \tag{2}$$

where $\Gamma_{r(Na)} = \rho_{Na}\mu_{Na}\mathrm{E}_r - D_{Na}\frac{\partial \rho_{Na}}{\partial r}$ and $\Gamma_{z(Na)} = \rho_{Na}\mu_{Na}\mathrm{E}_z - D_{Na}\frac{\partial \rho_{Na}}{\partial z}$.

$$\frac{\partial \rho_{Cl}}{\partial t} + \nabla . \boldsymbol{\Gamma}_{Cl} = 0 \tag{3}$$

where $\Gamma_{r(Cl)} = \rho_{Cl}\mu_{Cl}\mathrm{E}_r - D_{Cl}\frac{\partial \rho_{Cl}}{\partial r}$ and $\Gamma_{z(Cl)} = \rho_{Cl}\mu_{Cl}\mathrm{E}_z - D_{Cl}\frac{\partial \rho_{Cl}}{\partial z}$.

In the aforementioned equations, ρ, Γ, μ and D specify the electric charge density, the current density, the ion mobility and diffusion coefficients, respectively. Furthermore, standard values for sodium and chlorine ion mobility and diffusion coefficients are [27, 28]:

$\mu_{\mathrm{Na}} = 5.19\times10^{-8}\,\mathrm{m^2V^{-1}s^{-1}}, D_{\mathrm{Na}} = 1.33\times10^{-9}\,\mathrm{m^2s^{-1}},$

$\mu_{\mathrm{Cl}} = 7.91\times10^{-8}\,\mathrm{m^2V^{-1}s^{-1}}, D_{\mathrm{Cl}} = 2.03\times10^{-9}\,\mathrm{m^2s^{-1}}.$

It is worth noting that E_r and E_z can be computed as

$$E_r = -\frac{\partial}{\partial r}\Phi,$$

$$E_z = -\frac{\partial}{\partial z}\Phi,$$

where Φ satisfies the Poisson equation $\nabla^2\Phi = -\frac{e}{\varepsilon_r\varepsilon_0}\left(\rho_{Na} - |\rho_{Cl}|\right)$. Moreover, Φ is obtained by solving the Poisson and continuity equations coupled with the Navier-Stokes equation in the next section simultaneously. Therefore, first it is not assumed that Φ is definite.

It should be noted that the presence of the external potential is considered through the application of the boundary condition on the unit cell. In this paper, a time-dependent

potential difference is applied between two parallel-plate capacitive coupling electrodes. The electric field of 66 Vm^{-1} is considered to be applied along the symmetry axis of the system with a frequency of 1 GHz.

In the Poisson equation for the boundaries far enough from the macromolecule, the following boundary condition is valid

$$\mathbf{n}.\mathbf{D} = 0, \quad (4)$$

where **D** denotes the electric displacement vector [26].

A schematic view of the considered system is shown in fig. 1. The model considers a rod-like macromolecule associated with a coaxial unit cell. The z axis is selected as the common axis of the charged macromolecule and the unit cell. The inside of the unit cell includes the counter ions equivalent to the charges on the macromolecule. Therefore, the unit cell is electrically neutral.

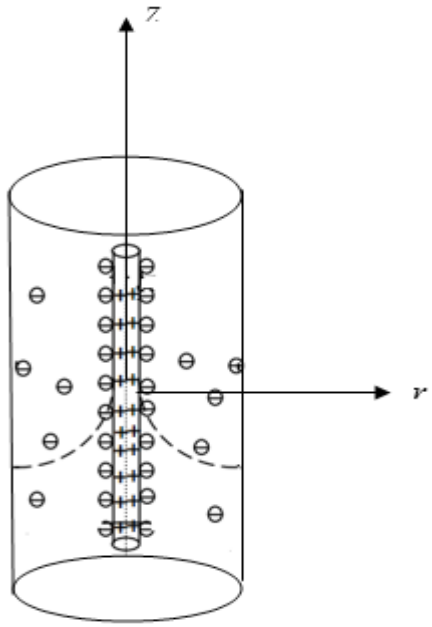

Fig. 1. The model considers a rod-like macromolecule associated with a coaxial unit cell

The radius and height of the macromolecule are selected as 0.5 nm and 12 nm [29], respectively, with the surface charge density [30]. Therefore, on the surface of the macromolecule, the following boundary condition has been used:

$$\mathbf{n}.(\mathbf{D}_1 - \mathbf{D}_2) = \sigma, \quad (5)$$

where *n* is normal unit vector to the surface from the region 2 to region 1. Furthermore, $\mathbf{D}_1$ and $\mathbf{D}_2$ denote the electric displacements for the inside as well as outside of the macromolecule, respectively. Moreover, σ shows the surface charge density of the macromolecule. The dielectric constant of the macromolecule is usually taken to be approximately 3 [31]. Moreover, an ion-exclusion region, the so-called Stern layer, is often added outside the molecular interior in order to mimic the effect of finite ion size. This region is supposed to contain water, and therefore has a high dielectric constant. To model the ion-exclusion effect for this region, the charge density in this region is set to be zero. The reason is that the ions are not able to approach the molecule closely due to the van der Waals repulsion between the ions and the biomolecule surface. However, molecular dynamics simulations indicate that ions can approach the biomolecule by their roughly van der Waals' radius. As a result, the thickness of the Stern layer can be attributed to the van der Waals' radius of the largest counter ion in a solution, which is considered to be as 0.3 nm in our calculations [29]. The exterior region with a charge distribution represents the free ions in a solution. The continuity equations for the positive and negative ions coupled with Poisson's equation in this region are simultaneously solved.

In the continuity equation, the Dirichlet boundary condition has been used for the unit cell. Moreover, the continuity of the normal component of the electric current density is applied in the interface of the macromolecule and its surrounding.

For the convergence test and to achieve sufficient accuracy, the selected triangular mesh in FEM should be sufficiently small. The number of equations to be solved in this study is equal to 17889. In our simulations, the mesh consists of 1511 nodes and 2942 elements. Furthermore, the number of boundary elements is 206. Besides, the time steps are selected small enough so that considering smaller time steps does not change the final results noticeably. For more details, the time steps are taken as $0.1T$, where T is the time period of the external field.

2- 2- Navier-Stokes equation for fluid dynamics

To take into account the electroosmotic flow, incompressible fluid flow is described by the Navier-Stokes and continuity equations, which are shown by eqs. (6) and (7), respectively [22].

$$\rho\left(\frac{\partial \mathbf{v}}{\partial t} + \mathbf{v}.\nabla v\right) = -\nabla p + \eta\nabla^2 v - (\rho_{Na^+} - \rho_{Cl^-})\nabla\Phi \quad (6)$$

$$\nabla.\mathbf{v} = 0. \quad (7)$$

The sodium and chlorine ion densities as well as the electric potential are obtained by solving the Poisson, continuity and Navier-Stokes equations simoultaneously. In other words, ρ_{Na}, ρ_{Cl} and Φ are the output of the equations in the sections 2.1 and 2.2.

In the aforementioned equation v, p, $\eta = 0.002\,\text{Pa.s}$ and $\rho = 1000\,\text{kg/m}^3$ are velocity, pressure, viscosity and density, respectively [22]. The assumption of incompressibility is not generally applicable to all microfluidic systems. Anyway, as most electroosmotic flows tend to involve a single phase liquid, this assumption can be made without loss of generality. The Navier-Stokes equation makes a mathematical model of the motion of a fluid which is important in the study of fluid dynamics.

It is worth mentioning that the solution of equations (6) and (7) can result in the velocity. This velocity is relevant to the water i.e. fluid. In fact, the opposite charges are adsorbed to the surface of the macromolecule due to its intrinsic surface charge. These charges make a layer of the net charge in the vicinity of the macromolecule. It is notable that due to the motion of the net charge, the pressure is created in the fluid, the so-called the electroosmotic flow.

The last term in eq. (6) denotes the electroosmotic body force, and it is equal to the product of the net charge density in the EDL, multiplied by the gradient of the total potential, Φ. The potential of EDL and the net charge density are related by the Poisson equation, namely eq. (1). Moreover, the continuity equations are presented for sodium and chlorine ions as eqs. (2) and (3). The no-slip boundary condition as $v = 0$ has been used in this analysis for the macromolecule and the unit cell.

It is notable that the number of equations to be solved in this study is considered as 31326.

2- 3- Verification of the model

The response of a material to an electromagnetic wave is described by the frequency dependent complex permittivity $\varepsilon = \varepsilon' - i\,\varepsilon''$ for which the imaginary part is proportional to the spectral absorption power [32]. Both Debye and Cole–Cole models have been used to describe the dielectric behavior of NaCl solutions. It has been found that the Debye expression becomes more appropriate for NaCl solutions with low concentration, namely less than 0.5 mol/L, while for higher concentrations the Cole-Cole model is preferred [33].

The complex dielectric constant $\varepsilon^*(\omega)$ is usually written as [34]

$$\varepsilon^*(\omega) = \varepsilon'(\omega) + \frac{\sigma(\omega)}{i\,\varepsilon_0 \omega}, \tag{8}$$

where ω, $\varepsilon'(\omega)$ and $\sigma(\omega)$ are the angular frequency, the real part of the complex dielectric constant and the conductivity, respectively. The dielectric loss $\sigma(\omega)/\varepsilon_0\omega$ consists of two components. One is due to the dielectric process $\varepsilon''(\omega)$, whereas the other one is related to the dc electrical conductivity σ_0, *i.e.* the low-frequency limit of $\sigma(\omega)$. The general expression of eq. (8) is then

$$\varepsilon^*(\omega) = \varepsilon'(\omega) - i\left[\varepsilon''(\omega) + \frac{\sigma_0}{\varepsilon_0 \omega}\right]. \tag{9}$$

The dielectric loss ε'' has been ignored in our model due to the negligible dispersion of the medium for 1 GHz. The current density due to the free charges is specified by [26]

$$\mathbf{J}_c = \sigma_i\,\mathbf{E}, \tag{10}$$

where σ_i denotes the ionic conductivity as follows:

$$\sigma_i = \rho_{Na^+}\mu_{Na^+}e + \rho_{Cl^-}\mu_{Cl^-}e. \tag{11}$$

The displacement current density is described by

$$\mathbf{J}_d = \varepsilon_r'\varepsilon_0\frac{\partial \mathbf{E}}{\partial t}, \tag{12}$$

where ε_r' specifies the relative dielectric constant of the water. Therefore, the total current density is approximated in the phasor form as follows

$$\mathbf{J}_{tot} = (\sigma_i + i\omega\varepsilon_0\varepsilon_r')\mathbf{E} + (\rho_{Na} - \rho_{Cl})\mathbf{v} = i\omega\varepsilon_0\left(\varepsilon_r' + \frac{\sigma_i}{i\omega\varepsilon_0}\right)\mathbf{E} + (\rho_{Na} - \rho_{Cl})\mathbf{v}. \tag{13}$$

The total current is defined by

$$I = \int \mathbf{J}_{tot}.\mathbf{ds} = \int i\,\omega\varepsilon_0\left(\varepsilon_r' + \frac{\sigma_i}{i\,\omega\varepsilon_0}\right)\mathbf{E}.\mathbf{ds} + \int(\rho_{Na} - \rho_{Cl})\mathbf{v}.\mathbf{ds}. \tag{14}$$

Afterward, we can compute the admittance as follows [26]

$$Y = I / V = i\,\omega\varepsilon_0\left(\varepsilon'_{r\,effec} + \frac{\sigma_{i\,effec}}{i\,\omega\varepsilon_0}\right)\frac{A}{d} + \frac{1}{V}\int(\rho_{Na} - \rho_{Cl})\mathbf{v}.\mathbf{ds}, \tag{15}$$

where $\left(\varepsilon'_{r\,effec} + \frac{\sigma_{i\,effec}}{i\,\omega\varepsilon_0}\right)$ stands for the effective complex permittivity. Besides, d and A are the distance between two electrodes and the surface of the electrode, respectively. Moreover, a sinusoidal electric potential is applied to the electrodes

$$V = V_{\max}\sin(2\pi f t) \tag{16}$$

First, the admittance was computed according to eqs. (14), (15) and (16). Afterwards, the effective complex permittivity was obtained. As a conclusion, the real and imaginary parts of the effective complex permittivity were calculated 73.43 and 3.61, respectively. We draw a conclusion that the complex permittivity is smaller in comparison with the experimental limits obtained for protein solution [33]. This conclusion is true because, on the one hand, the presence of the macromolecule can decrease the complex permittivity of the saline solution [35]. On the other hand, the dielectric loss has been ignored in this work, whereas it has been considered in [33]. It is notable that our computations show that the order of magnitude for $(\rho_{Na} - \rho_{Cl})\mathbf{v}$ is 10^{-10} compared to the term

$$(\sigma_i + i\,\omega\varepsilon_0\varepsilon_r')\mathbf{E} = i\,\omega\varepsilon_0\left(\varepsilon_r' + \frac{\sigma_i}{i\,\omega\varepsilon_0}\right)\mathbf{E}$$

which its order is 10^{-5}. Therefore, this result demonstrates that the electroosmotic flow has negligible influence on the counter ion number density.

It is notable that Poisson-Boltzmann equation (PBE) gives adequate descriptions regarding the steady-state electrostatic solutions [36-38]. In order to show that the FEM programming is working properly, the solution of the PBE with one variable in saline solution for a large plate by FEM is compared with the corresponding Gouy-Chapman solution. The PBE governing the steady state behavior of the electric potential in the saline solution is as follows [39, 40]:

$$\nabla^2\Phi = -\frac{e\rho_0}{\varepsilon_r\varepsilon_0}\left[\exp\left(-\frac{e\Phi}{k_B T}\right) - \exp\left(+\frac{e\Phi}{k_B T}\right)\right], \tag{17}$$

where ρ_0 is the average density of both sodium and chlorine ions in the solution. In general, this potential depends on the distance from the surface which is denoted by x.

An analytical solution of eq. (17) for a large plate corresponding to the surface of lipid droplets in saline as well as cell phospholipid bilayer membrane is found in the literature. The solution, the so-called Gouy–Chapman formula, is defined by [39]

$$\Phi = \frac{2k_B T}{e}\ln\left[\frac{1+\gamma e^{-kx}}{1-\gamma e^{-kx}}\right], \tag{18}$$

where

$$\gamma = \tanh\left(\frac{e\Phi_0}{4k_B T}\right) \tag{19}$$

and

$$k = \sqrt{\frac{2e^2\rho_0}{\varepsilon_r\varepsilon_0 k_B T}}. \tag{20}$$

Moreover, Grahame derived the following relationship between surface charge density σ and the surface potential Φ_0 based on the Gouy–Chapman theory [39].

$$\sigma = \sqrt{8\rho_0\varepsilon_r\varepsilon_0 k_B T}\,\sinh\left(\frac{e\Phi_0}{2k_B T}\right). \tag{21}$$

We use eq. (21) in order to obtain the potential of the macromolecule surface Φ_0 with a defined surface charge density σ [29, 30].

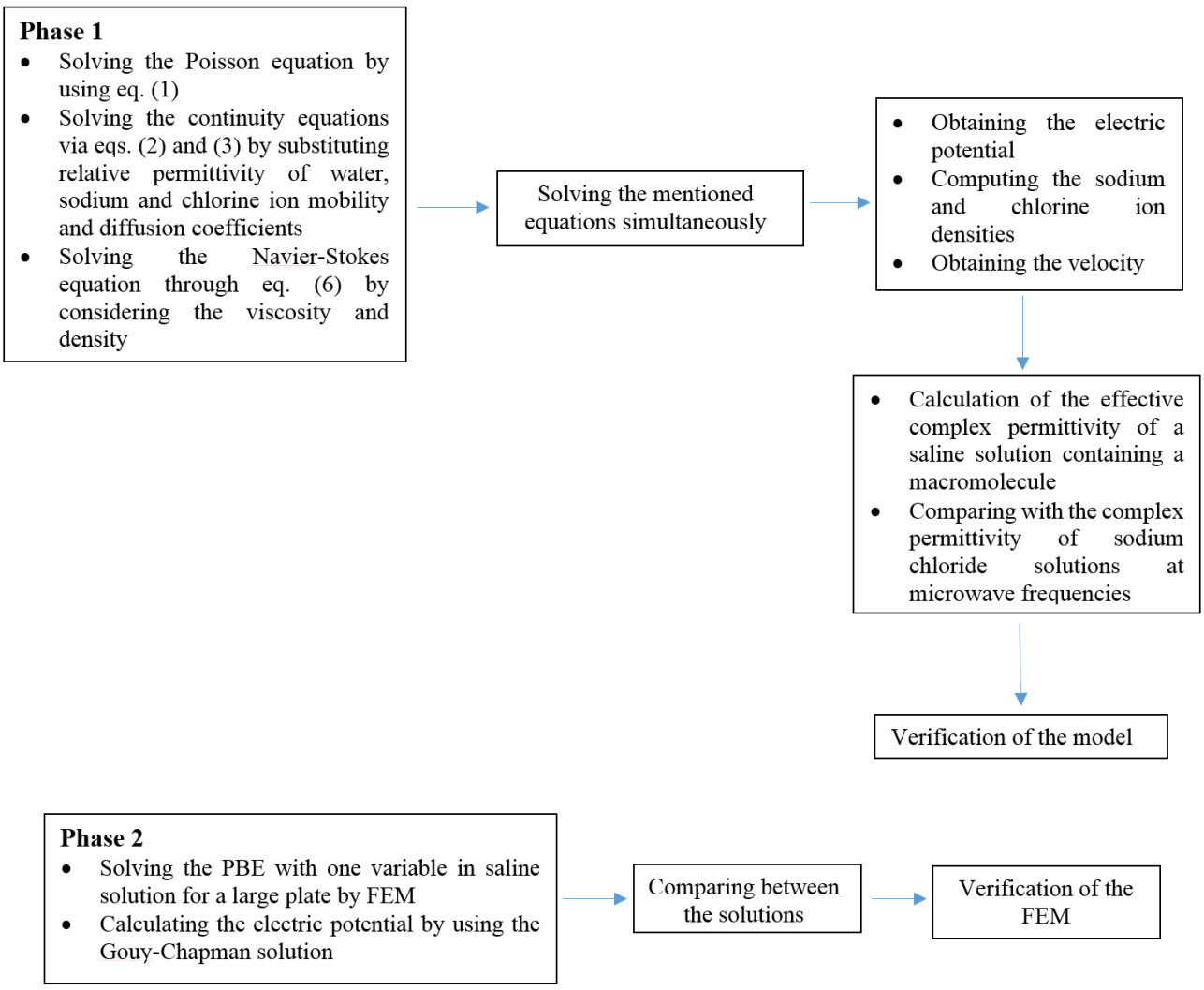

Finally, the above flowchart can be considered to make the computation mechanism easier to follow and understand.

It is notable that the computation mechanism can be summarized in the following steps for more clearance.

Step 1: The boundary conditions are specified in the Poisson equation as equation (4) for the boundaries far enough from the macromolecule and equation (5) on the surface of the macromolecule.

Step 2: The boundary conditions in the sodium and chlorine ion continuity equations are defined as the Dirichlet boundary condition for the unit cell. Furthermore, the normal component of the electric current density must be continuous in the interface of the macromolecule and its surrounding.

Step 3: The boundary conditions are specified in the Navier-Stokes equation in the form of the no-slip boundary condition as $v = 0$ for the macromolecule and the unit cell.

Step 4: The Poisson, continuity and Navier-Stokes equations are solved simultaneously for obtaining the electric potential, the sodium and chlorine ion densities and the velocity, respectively.

Step 5: The ionic conductivity is computed via equation (11) by substituting sodium and chlorine ion densities as well as the mobility coefficients.

Step 6: The total current density is computed through equation (13) by substituting the ionic conductivity, sodium and chlorine ion densities, electric field and velocity.

Step 7: The total current is computed by using equation (14).

Step 8: The admittance is computed via equation (15) by considering a sinusoidal electric potential applied to the electrodes.

Step 9: The effective complex permittivity of a saline solution containing a macromolecule is computed by ignoring the dielectric loss at frequency of 1 GHz.

Step 10: The electric potential is computed by using the PBE i.e. equation (17) with one variable in saline solution for a large plate based on FEM by considering the average density of both sodium and chlorine ions in the solution, the Boltzmann constant and temperature.

Step 11: The electric potential is computed through the Gouy-Chapman solution i.e. equation (18) by substituting the surface charge density σ and the defined parameters in the step 10.

Step 12: The FEM programming is verified by using the comparison between the solution of the PBE in the step 10 as well as the Gouy-Chapman solution in the step 11.

3- Numerical results and discussion

As presented in fig. 2, our numerical results are compared with the analytical solution of a PBE with one variable in saline solution. This case corresponds with a plate with a

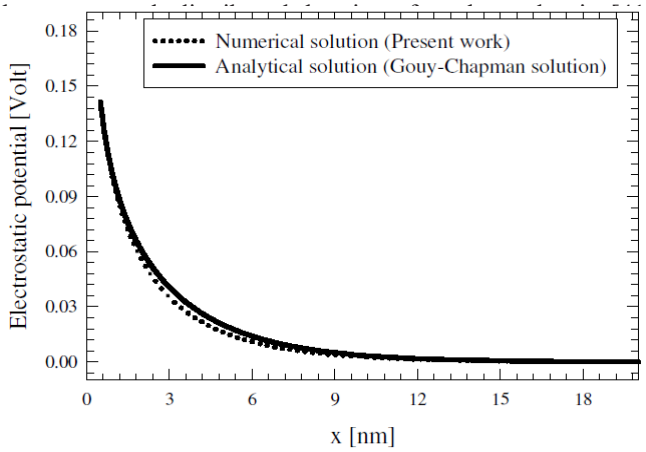

Fig. 2. The electrostatic potential obtained from the Gouy-Chapman solution [39] compared with our numerical method for a large plate, in the saline solution, which corresponds to one variable PBE.

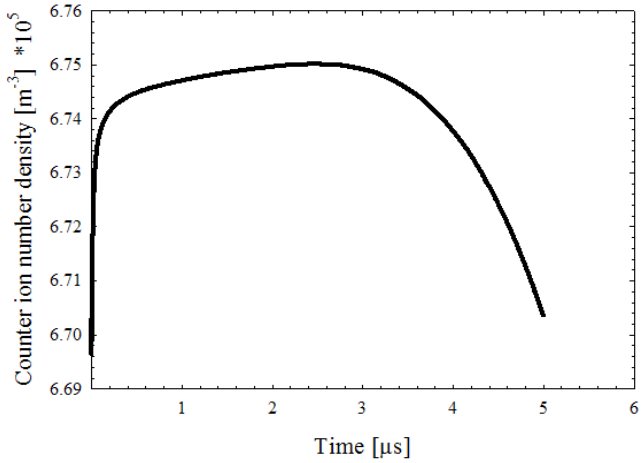

Fig. 3. The density of counter ions as a function of time at r = 4 nm and z = 0 after applying external electric field with the amplitude of 66 Vm^{-1} and the frequency of 1 GHz

that for the times larger than 2.7 μs, the aggregation of the counter ions decreases. In fact, the external field makes a reduced aggregation of the ion atmosphere. Following this decrement, the mobility of the counter ions along the field gradient increases [29]. This observation can be considered as the cause of the Debye-Falkenhagen effect. This conclusion is in agreement with the experimental result reported in the literature [9], so that the EMF exposure of a luciferase molecule results in its reduced aggregation. This can be due to the real and imaginary parts of the permittivity before and after exposure. The real part of the permittivity reduces in low frequency and increases in high frequency after exposure. The status is inverse in the case of the imaginary part of the permittivity so that the imaginary part of the permittivity reduces in high frequency and increases in low frequency after exposure. Since ionic content is decisive in the case of the imaginary part in the low-frequency, some ions become free of the protein structure and are added to the system. It should be noted that the bound ions to the system create the real part. Therefore, when the bound ions are released, a component of the polarization is reduced. As a result, the ions around the protein are reduced. In fig. 3, the steep slope of the density is up to 0.1 μs due to the formation of the counter ion cloud around the macromolecule. Afterwards, up to 2.7 μs, the slope of the density changes slower. This behavior can be explained by the effect of the repulsive force among the accumulated counter ions located at the end of the macromolecule. From 2.7 μs, the effect of the field is quite obvious. In other words, due to the application of the field, the opposite ions move along the field and are accumulated around the cylindrical bases (macromolecule). Therefore, the sum of surface charges associated with opposite ions decreases around the macromolecule on its lateral surface.

Moreover, in the case of fig. 3, it can be probably concluded that, due to the nonlinear processes (a set of the nonlinear equations) as well as the inertia of the charges, the variations of the charge distribution do not follow the velocity of the electric field. One can see that the charge distribution indicates the slower dynamics rather than the electric field as the order of microseconds.

Figure 4 shows the density of the counter ions at the distance 4 nm from the axis of the macromolecule for nine time instants. One can observe that concentration of the counter ions becomes larger near the center of the macromolecule as time elapses. For $t = 1.5$ μs, the broadening of the distribution is smaller than the computed one for other time instants. However, the maximum of the distributions corresponds with the center of the macromolecule for all the times computed in this analysis. As shown, for the times larger than 2.7 μs, the distribution of the counter ions decreases. It should be noted that this analysis is able to predict how the ion atmosphere can be affected by the electric fields. It is notable that the ion distribution is perturbed by the applied electric field. Consequently, the local conductivity can be influenced by the external electric field, and hence, the equation governing the Ohm's law is no longer linear. Therefore, the continuity equations, coupled with the Poisson's equation analyzed in this work, constitute a set of the nonlinear equations, whereas the dielectric coefficient behaves linearly.

4- Conclusion

In this work, the time evolution of the charge density distribution was obtained in a saline solution containing a rodlike macromolecule. The charge density was simultaneously computed by solving ion continuity equations coupled with Poisson's equation based on the FEM. It was concluded that as time elapsed, the counter ions accumulated near the center of the macromolecule, namely $z = 0$. The external field made a reduced aggregation of the ion atmosphere for the times larger than 2.7 μs. Our result showed a satisfactory consistency with the experimental one [9] so that the aggregation of the ion atmosphere was reduced by the external electric field. Besides, our results were in excellent agreement with the analytical solution for one dimensional PBE. Furthermore, the real and imaginary parts of the effective complex permittivity were computed as 73.43 and 3.61 by considering electroosmotic flow, respectively. It is worth noting that the obtained data were in agreement with the experimental limits [33]. In fact, the presence of the macromolecule could decrease the complex permittivity of the saline solution [35]. Furthermore, it was concluded that the electroosmotic flow could not affect the density of counter ions significantly, and hence it could be neglected. It is notable that the study of the effects of time varying electric fields in the biological tissue is applicable for the protein aggregation disorders.

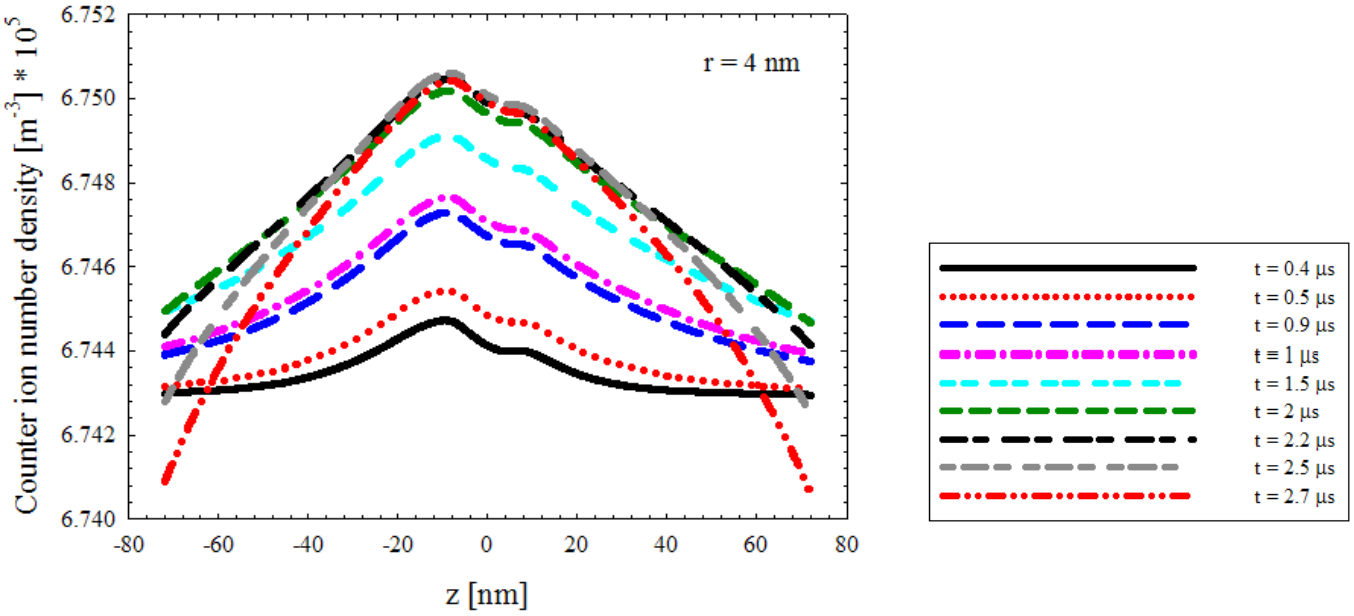

Fig. 4. The counter ion number density as a function of z for nine time instances at r = 4 nm, in the presence of external electric field with the amplitude of 66 Vm^{-1} and the frequency of 1 GHz. The computed data are illustrated in the figure.

References

[1] L. Dubois, J.-P. Sozanski, V. Tessier, J.-C. Camart, J.-J. Fabre, J. Pribetich, M. Chive, Temperature control and thermal dosimetry by microwave radiometry in hyperthermia, IEEE Transactions on Microwave Theory and Techniques, 44(10) (1996) 1755-1761.

[2] D. Dunn, C.M. Rappaport, A. Terzuoli, FDTD verification of deep-set brain tumor hyperthermia using a spherical microwave source distribution, IEEE transactions on microwave theory and techniques, 44(10) (1996) 1769-1777.

[3] C. Rappaport, F. Morgenthaler, Optimal source distribution for hyperthermia at the center of a sphere of muscle tissue, IEEE transactions on microwave theory and techniques, 35(12) (1987) 1322-1327.

[4] C. Rappaport, J. Pereira, Optimal microwave source distributions for heating off-center tumors in spheres of high water content tissue, IEEE transactions on microwave theory and techniques, 40(10) (1992) 1979-1982.

[5] D. Sullivan, Three-dimensional computer simulation in deep regional hyperthermia using the finite-difference time-domain method, IEEE transactions on microwave theory and techniques, 38(2) (1990) 204-211.

[6] A. Vander Vorst, F. Duhamel, 1990-1995 Advances in investigating the interaction of microwave fields with the nervous system, IEEE transactions on microwave theory and techniques, 44(10) (1996) 1898-1909.

[7] F. Apollonio, G. d'Inzeo, L. Tarricone, Theoretical analysis of voltage-gated membrane channels under GSM and DECT exposure, in: Microwave Symposium Digest, 1997., IEEE MTT-S International, IEEE, 1997, pp. 103-106.

[8] J.C. Lin, S.M. Michaelson, Biological effects and health implications of radiofrequency radiation, Springer Science & Business Media, 2013.

[9] Y. Sefidbakht, S. Hosseinkhani, M. Mortazavi, I. Tavakkolnia, M.R. Khellat, M. Shakiba-Herfeh, M. Saviz, R. Faraji-Dana, A.A. Saboury, N. Sheibani, Effects of 940 MHz EMF on luciferase solution: Structure, function, and dielectric studies, Bioelectromagnetics, 34(6) (2013) 489-498.

[10] O. Grigore, O. Calborean, G. Cojocaru, R. Ungureanu, M. Mernea, M. Dinca, S. Avram, D. Mihailescu, T. Dascalu, High-intensity THz pulses application to protein conformational changes, Romanian Reports in Physics, 67(4) (2015) 1251-1260.

[11] F. Belloni, D. Doria, A. Lorusso, V. Nassisi, L. Velardi, P. Alifano, C. Monaco, A. Talà, M. Tredici, A. Rainò, Experimental analysis of a TEM plane transmission line for DNA studies at 900 MHz EM fields, Journal of Physics D: Applied Physics, 39(13) (2006) 2856.

[12] J.K. Dhont, K. Kang, Electric-field-induced polarization of the layer of condensed ions on cylindrical colloids, The European Physical Journal E, 34(4) (2011) 40.

[13] S. Fischer, R. Netz, Low-frequency collective exchange mode in the dielectric spectrum of salt-free dilute polyelectrolyte solutions, The European Physical Journal E, 36(10) (2013) 117.

[14] R. Gan, W. Yan-Ting, Saturated sodium chloride solution under an external static electric field: A molecular dynamics study, Chinese Physics B, 24(12) (2015) 126402.

[15] J. Hand, Modelling the interaction of electromagnetic fields (10 MHz–10 GHz) with the human body: methods and applications, Physics in Medicine & Biology, 53(16) (2008) R243.

[16] F.X. Hart, Cytoskeletal forces produced by extremely low-frequency electric fields acting on extracellular glycoproteins, Bioelectromagnetics: Journal of the Bioelectromagnetics Society, The Society for Physical Regulation in Biology and Medicine, The European

Bioelectromagnetics Association, 31(1) (2010) 77-84.

[17] S. Takashima, C. Gabriel, R. Sheppard, E. Grant, Dielectric behavior of DNA solution at radio and microwave frequencies (at 20 degrees C), Biophysical journal, 46(1) (1984) 29-34.

[18] T. Vreugdenhil, F. Van der Touw, M. Mandel, Electric permittivity and dielectric dispersion of low-molecular weight DNA at low ionic strength, Biophysical chemistry, 10(1) (1979) 67-80.

[19] M.N. Sadiku, A simple introduction to finite element analysis of electromagnetic problems, IEEE Transactions on Education, 32(2) (1989) 85-93.

[20] A. Deshkovski, S. Obukhov, M. Rubinstein, Counterion phase transitions in dilute polyelectrolyte solutions, Physical review letters, 86(11) (2001) 2341.

[21] R. Morrow, D. McKenzie, M. Bilek, The time-dependent development of electric double-layers in saline solutions, Journal of Physics D: Applied Physics, 39(5) (2006) 937.

[22] V.P. Andreev, Cytoplasmic electric fields and electroosmosis: possible solution for the paradoxes of the intracellular transport of biomolecules, PloS one, 8(4) (2013) e61884.

[23] R. Hossain, K. Adamiak, Dynamic properties of the electric double layer in electrolytes, Journal of Electrostatics, 71(5) (2013) 829-838.

[24] P.J. Roache, Computational fluid dynamics, Hermosa publishers, 1972.

[25] D.J. Griffiths, Electrodynamics, Introduction to Electrodynamics, 3rd ed., Prentice Hall, Upper Saddle River, New Jersey, (1999) 301-306.

[26] J.D. Jackson, Classical electrodynamics, John Wiley & Sons, 2012.

[27] A. Adamson, A textbook of physical chemistry, Elsevier, 2012.

[28] P. Atkins, J. De Paula, J. Keeler, Atkins' physical chemistry, Oxford university press, 2018.

[29] M. Yoshida, K. Kikuchi, T. Maekawa, H. Watanabe, Electric polarization of rodlike polyions investigated by Monte Carlo simulations, The Journal of Physical Chemistry, 96(5) (1992) 2365-2371.

[30] M.L. Bret, B.H. Zimm, Distribution of counterions around a cylindrical polyelectrolyte and Manning's condensation theory, Biopolymers: Original Research on Biomolecules, 23(2) (1984) 287-312.

[31] E. Grant, The dielectric method of investigating bound water in biological material: An appraisal of the technique, Bioelectromagnetics: Journal of the Bioelectromagnetics Society, The Society for Physical Regulation in Biology and Medicine, The European Bioelectromagnetics Association, 3(1) (1982) 17-24.

[32] S. Gekle, R.R. Netz, Nanometer-resolved radio-frequency absorption and heating in biomembrane hydration layers, The Journal of Physical Chemistry B, 118(18) (2014) 4963-4969.

[33] A. Peyman, C. Gabriel, E. Grant, Complex permittivity of sodium chloride solutions at microwave frequencies, Bioelectromagnetics: Journal of the Bioelectromagnetics Society, The Society for Physical Regulation in Biology and Medicine, The European Bioelectromagnetics Association, 28(4) (2007) 264-274.

[34] F. Bordi, C. Cametti, R. Colby, Dielectric spectroscopy and conductivity of polyelectrolyte solutions, Journal of Physics: Condensed Matter, 16(49) (2004) R1423.

[35] H.P. Schwan, Interaction of microwave and radio frequency radiation with biological systems, IEEE Transactions on microwave theory and techniques, 16(2) (1971) 146-152.

[36] S. Nikzad, H. Noshad, Electrostatic analysis of the charged surface in a solution via the finite element method: The Poisson-Boltzmann theory, AUT Journal of Electrical Engineering, 48(1) (2016) 11-17.

[37] S. Nikzad, H. Noshad, E. Motevali, Study of nonlinear Poisson-Boltzmann equation for a rodlike macromolecule using the pseudo-spectral method, Results in physics, 7 (2017) 3938-3945.

[38] S. Nikzad, H. Noshad, M. Saviz, Steady state behavior of a finite rodlike macromolecule in salt free solution, Results in physics, 7 (2017) 2658-2662.

[39] H.-J. Butt, H.-J.B. Butt, K. Graf, M. Kappl, Physics and chemistry of interfaces, John Wiley & Sons, 2003.

[40] A. Majee, M. Bier, S. Dietrich, Poisson-Boltzmann study of the effective electrostatic interaction between colloids at an electrolyte interface, The Journal of Chemical Physics, 145(6) (2016) 064707.

[41] D. Murray, A. Arbuzova, G. Hangyás-Mihályné, A. Gambhir, N. Ben-Tal, B. Honig, S. McLaughlin, Electrostatic properties of membranes containing acidic lipids and adsorbed basic peptides: theory and experiment, Biophysical Journal, 77(6) (1999) 3176-3188.

[42] R.M. Peitzsch, M. Eisenberg, K.A. Sharp, S. McLaughlin, Calculations of the electrostatic potential adjacent to model phospholipid bilayers, Biophysical journal, 68(3) (1995) 729-738.

Please cite this article using:

Sh. Nikzad, H. Noshad, M. Saviz, Response of A Saline Solution Containing A Macromolecule To An External Electric Field, *AUT J. Elec. Eng.*, 50(2) (2018) 121-128.

DOI: 10.22060/eej.2018.13703.5181